FORMING OF POLYPROPYLENE FILM WITH THE ADDITION OF DIBUTYRYLCHITIN AND STEARIC ACID

Dorota Biniaś

Institute of Engineering Sciences, Faculty of Materials, Civil and Environmental Engineering, University of Bielsko-Biala, Willowa 2 Str., 43-309 Bielsko-Biała, Poland
ORCID: 0000-0002-2548-1774
corresponding author: dbinias@ubb.edu.pl

Abstract

In this work, polypropylene (PP) films with varying percentages of dibutyrylchitin (DBC) and stearic acid (SA) were prepared. In the first stage, the PP film was treated with diisopropyl ether to extract stearic acid, resulting in a porous structure of the PP film containing the DBC additive. Only stearic acid was washed out, as the diisopropyl ether is not a DBC solvent. In the next stage, the film was treated with a 5% potassium hydroxide solution to convert DBC into chitin and to convert any remaining SA into potassium stearate (SP). Washing out the resulting SP with distilled water yielded porous PP film with chitin and its derivative of DBC. Chemical changes occurring during processing were examined using Fourier Transform Infrared Spectroscopy (FTIR). The morphology of the film surface at consecutive processing stages was imaged using microscopic methods: scanning electron microscopy (SEM) and optical microscopy (OM). After solidification of the PP polymer matrix, the applied SA crystallises on the surface of the PP film. As a result of the applied procedure, the PP film with the addition of DBC and chitin was obtained. It is anticipated that this bioactive material can be used in medicine, e.g., as a wound dressing, hernia mesh, or scaffolds.

Keywords: *polypropylene, dibutyrylchitin, porous film, FTIR spectroscopy*

Received: 03.04.2025
Accepted: 26.06.2025

1. Introduction

Polypropylene (PP) is a semi-crystalline polymer of the polyolefin group. The properties of PP depend on the molecular weight and its distribution and on the degree of crystallinity [1, 2]. It is a light polymer with a density of 0.90 g/cm^3 suitable for many industrial applications, as it has good chemical resistance, good mechanical, thermal, and optical properties, as well as a long service life in electrical applications [3, 4]. PP is a thermoplastic polymer; thus, it can be easily processed into fibre, film, membrane, or a composite. The PP products are used in environmental protection and engineering as filters, in the food industry as packaging, in construction as insulating materials, and in medicine as dressings, surgical materials (such as filling materials including hernia meshes [5–9]), or in tissue engineering (TE) as scaffolds or drug carriers.

In the case of tissue engineering (TE), where the primary goal is to replace organs or restore specific cellular functions, natural materials, such as polysaccharides and polypeptides, are used to obtain functional materials [10].

The antibacterial activity of materials is usually obtained by physical or chemical treatment with appropriate compounds having adequate bioactive properties. One of the compounds with very good bioactive properties is chitin and its derivative, chitosan. Chitin exhibits high antimicrobial activity, biocompatibility, biodegradability, and low immunogenicity. The presence of chitin in a dressing accelerates wound healing, reduces scars, prevents inflammation and osteoporosis, and strengthens the body's immunity without any side reactions [11–14].

Chitin, second only to cellulose, is the most common polysaccharide on Earth. Due to its compact structure, chitin is insoluble in common organic solvents, which radically limits its direct use. The improvement of chitin solubility can be achieved by chemical modification, which leads to the formation of various derivatives. Dibutyrylchitin (DBC) is an ester derivative that can be obtained by esterification of natural chitin with butyric anhydride in the presence of perchloric acid [15–17]. DBC is readily soluble in commonly used organic solvents and, therefore, can be used to obtain biomaterials [18–21]. DBC exhibits biological properties such as biocompatibility, lipid solubility, biodegradability, and chitin regeneration; therefore, its use in wound dressings or as scaffolds for cartilage and bone repair has been investigated [22–24]. DBC can also be used as an additive to other polymers to render them bioactive properties. Examples are electrospun poly(lactic acid) (PLA) and DBC [25, 26].

This article presents a method of obtaining PP films with the addition of a chitin derivative that has not been described in the literature. The obtained PP-DBC material can be used in medicine as a dressing and surgical material, and in tissue engineering as scaffolds.

The aim of the research was to obtain microporous PP films with the addition of DBC and to perform alkaline treatment for the regeneration of the DBC component to chitin. Fourier transform infrared spectroscopy (FTIR) was used to examine chemical changes occurring during the treatment, and optical microscopy (OM) and scanning electron microscopy (SEM) were used to examine the surface morphology of the obtained films.

2. Materials and Methods

2.1. Materials

The commercial isotactic polypropylene PP, Moplen HP 462R, produced by Lyondell Basell Industries Holdings (The Netherlands), characterised by a melt flow index of 25 g/10 min, was used. Stearic acid (SA, $C_{18}H_{36}O_2$) and diisopropyl ether ($C_6H_{14}O$) were

supplied by POL-AURA (Zabrze, Poland), potassium hydroxide and acetone by Chempur (Piekary Śląskie, Poland). Dibutyrylchitin, DBC $(C_{14}H_{27}O_7N)_n$ of Mw = 160 kDa, was synthesised at the Department of Mechanical Engineering, Informatics and Chemistry of Polymer Materials, Łódź University of Technology. It was synthesised from chitin originating from shrimp shells (practical grade powder, Sigma-Aldrich Co. LLC., US) through esterification with butyric anhydride. DBC was characterised by 97.8% of acetylation and an intrinsic viscosity of 1.35 dl/g determined for its solution in acetone at 25°C. The chemical structures of the components are shown in Figure 1.

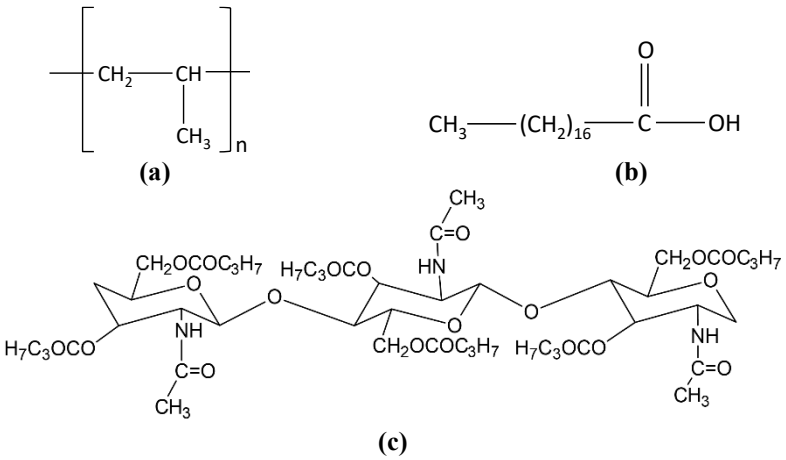

Figure 1. The chemical structure of reactants and the product: (a) PP, (b) SA, (c) DBC.

2.2. Methods

2.2.1. Preparation of Films and Alkaline Treatment

DBC and SA were dissolved in acetone. An appropriate amount of PP granulate was added to the solution. The solution was mixed with a mechanical stirrer at 60°C (Figure 2) until the solution-derived DBC and SA became evenly distributed on the surface of the PP granulate and the acetone evaporated. In this way, PP granulate coated with SA and DBC was obtained, which was then melted in an extruder (PROMA, Poland) at 170°C. As a result, homogeneous blends of PP and SA with the addition of DBC were obtained (Table 1), which served as the basis for forming the film.

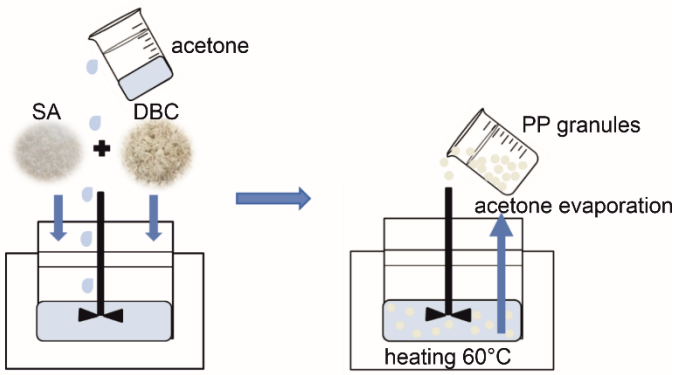

Figure 2. Schematic diagram of the preparation of PP granulate with additives for extrusion compounding and film manufacturing.

Table 1. Composition of DBC/SA/PP blends.

Sample	DBC [%]	SA [%]	PP [%]
1	0.0	10.0	90.0
2	5.0	10.0	85.0
3	5.0	20.0	75.0
4	7.5	10.0	82.5
5	10.0	20.0	70.0

The blends were pressed into film in laboratory conditions using a moulding press, Elcometer K 8400 (SciTeeX, Poland). All foils of 0.15 to 0.25 mm thickness were obtained using the same technological parameters: a pressure of 500 kG at a temperature of 165°C for 2 min. The films obtained with different contents of the additives were treated in diisopropyl ether to selectively remove SA, whereas DBC remained intact. Subsequently, the films were subjected to alkaline treatment in a 5% KOH solution and rinsed several times with water. The alkaline treatment aimed to convert DBC in the polymer matrix to chitin.

2.3. Analytical Methods

2.3.1. FTIR Spectroscopic Measurements

The spectroscopic investigations were carried out using a Nicolet 6700 Fourier Transform Infrared spectrophotometer (Thermo Scientific, Waltham, MA, USA) equipped with a photoacoustic MTEC model 300 accessory (Thermo Scientific, Waltham, MA, USA). OMNIC 9.0 software was applied to analyse the raw data. For photoacoustic testing, samples were placed in a dedicated snap holder. The spectral region was 4000 - 500 cm^{-1}, with a resolution of 4 cm^{-1}, 64 scans were done for the solid samples. Each spectrum was analysed using a linear baseline and pre-processed by means of Fourier smoothing.

The distribution of the applied additives inside and on the surface of the film was studied using a Nicolet 6700 Fourier Transform spectrophotometer (Thermo Scientific, Waltham, MA, USA) with an IR CONTINUUM microscope (Thermo Scientific, Waltham, MA, USA) employing the spectral map method. The band intensity distribution at the maximum position of 1740 cm^{-1} is characteristic of ester groups occurring only in DBC.

2.3.2. Morphology Analysis

The morphology analysis was performed using scanning electron microscopy (SEM, JSM 5500 LV, JEOL, Tokyo, Japan). The microscope was operating in back-scattered electron mode, using an accelerating voltage of 10 kV. The samples were gold-coated in a JEOL JFC 1200 (Tokyo, Japan) ion sputter coater.

The sample surface was also examined by an optical microscope (OM) (Reichert, Vienna, Austria) equipped with an ARTCAM CCD camera (Olympus, Tokyo, Japan), controlled by the Motic Images Plus 2.0 computer program.

3. Results and Discussion

The interactions of the PP, SA, and DBC components in DBC/SA/PP films were investigated using FTIR spectroscopy. Wavenumbers characteristic of PP, SA, and DBC are labelled in Table 2. Figure 3 shows the individual spectra of PP, SA, DBC, and the

spectrum of an exemplary film with the composition of 10% DBC, 20% SA, 70% PP (Table 1, sample 5), with the characteristic oscillation bands indicated.

Table 2. Wavenumbers of the bands in the FTIR spectra of PP, SA, DBC, chitin, and SP [27–31].

Sample	Wavenumber from FTIR [cm^{-1}]	Oscillation bands
PP	1454	CH_3 asym.
	1410	CH_3 asym.
	1378	CH_3 sym.
	1302	CH_3 sym.
	1166	C−C str.; C−C in CH_3 rock.
	998	CH_3 rock.
	972	CH_3 rock.; C−C str.
	900	CH_3 rock.; C−C str.
	842	C−H rock
	807	C−C str. CH_2 rock.
SA	1699	C=O
	1463	CH_2 asym.
	1430	CH_2 asym.
	1296	CH_2 sym.
	1240	C−O
	1220	C−O
	1200	C−O
	943	CH_2 rock.; C−C str
	807	C−C str. CH_2 rock.
	723	C−H
	688	C−H
DBC	1740	C=O
	1668	Amide I (C=O)
	1540	Amide II (C−N)
	1459	C−H
Chitin	1660	Amide I (C=O)
	1625	Amide I (C=O)
	1558	Amide II (C−N)
	1380	C−H sym.
	1314	Amide III (C−N)
	1260	CH_2 sym.
	1204	C−O
	1157	C−O
	1116	C−O
	1074	C−O
	953	CH_2 rock.; C−C str
	897	C−H rock
	718	C−C
SP	2930	CH_2 str. asym.
	2851	CH_2 str. sym.
	1576	C=O
	1465	CH_2 sc.
	1417	CH_3 sc.
	1003	C−C sk.

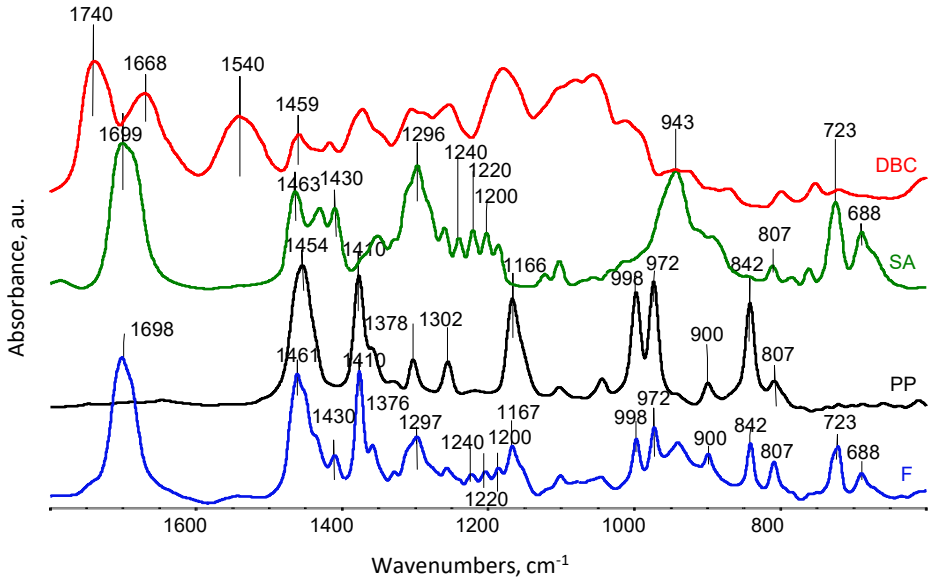

Figure 3. FTIR spectra of DBC, SA, PP, and the sample 5 film (F; 10% DBC, 20% SA, 70% PP).

The PP spectrum is characterised by peaks at the maximum band positions of 1454, 1410, 1302, 1166, 998, 972, 900, 842, and 807 cm^{-1}, consistent with the oscillation descriptions in Table 2. The SA spectrum is characterised by peaks at the maximum band positions of 1699, 1463, 1296, 1240, 1220, 1200, 943, 807, 723, and 688 cm^{-1}, consistent with the oscillation descriptions in Table 2. In the spectrum of the film, in addition to the major bands originating from the PP at maximum positions of 1410, 1376, 1297, 1167, 998, 972, 900, 842, and 807 cm^{-1}, bands characteristic of SA are visible at 1698, 1461, 1240, 1220, 1200, 723, and 688 cm^{-1}. During the film formation, the mixture phases separate. Firstly, as PP solidifies, SA, together with DBC, is separated in the form of flakes on the surface of PP spheres or is occluded within them. In the FTIR spectra for DBC/SA/PP films, the bands corresponding to DBC are not visible. At this stage, DBC is dispersed in PP and SA, and its bands are superimposed by the stronger bands of SA and PP. DBC bands become visible after the film is treated in diisopropyl ether and the SA is partially extracted (Figure 4).

Removing stearic acid crystals from the film's surface is clearly visible in SEM photographs. Figure 5 shows the film before and after stearic acid extraction, respectively. The SA flakes precipitated on the film surface are dissolved during the extraction process from the film with diisopropyl ether. SEM photograph of the film after extraction (Figure 5b) shows free spaces and microinclusions of DBC.

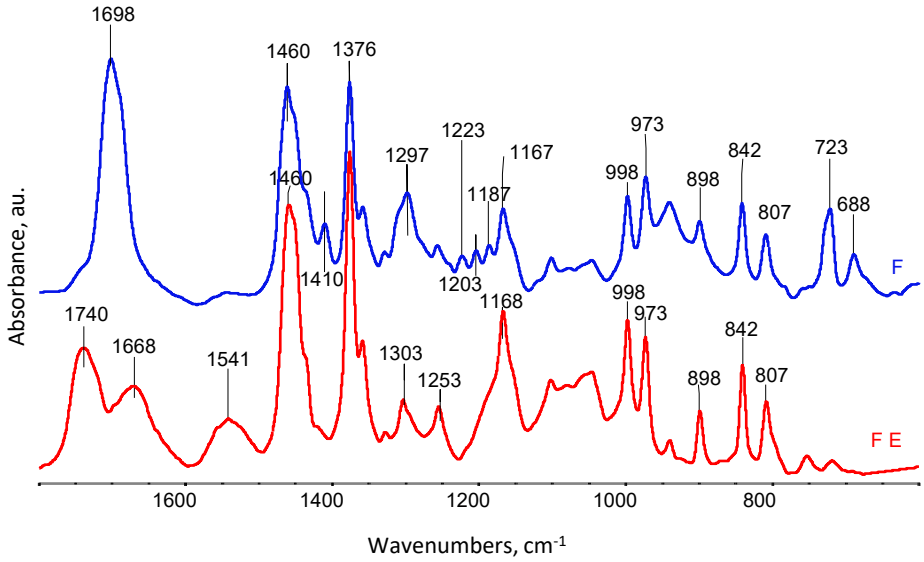

Figure 4. FTIR spectra of the sample 5 films (10% DBC, 20% SA, 70% PP) before (F) and after (FE) stearic acid extraction.

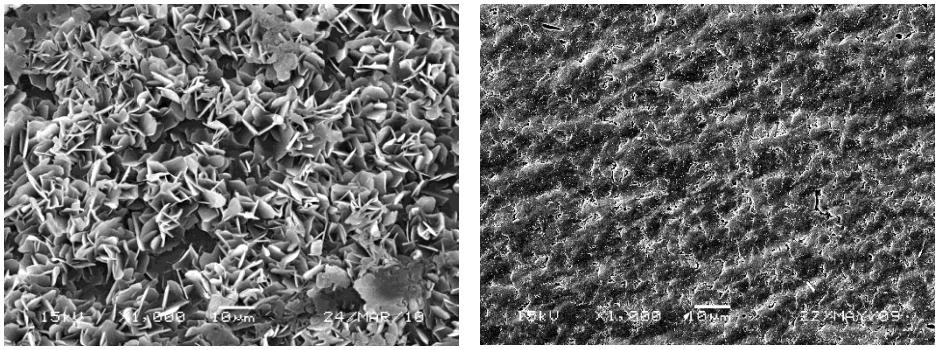

(a) **(b)**

Figure 5. SEM photographs of the sample 5 films (10% DBC, 20% SA, 70% PP) (a) before and (b) after SA extraction.

The surface morphology of the films was also examined using optical microscopy (Figure 6). Significant difference in the appearance of the films results from the specific optical properties of the free space within the PP matrix. Depending on the microstructure of the micropore surface, they interact specifically with visible radiation. The fundamental differences in the observed samples are caused by the extraction of SA (Figure 6b), which crystallises in the form of flakes (Figure 6a) and scatters light in a specific direction, that can be observed under the optical microscope.

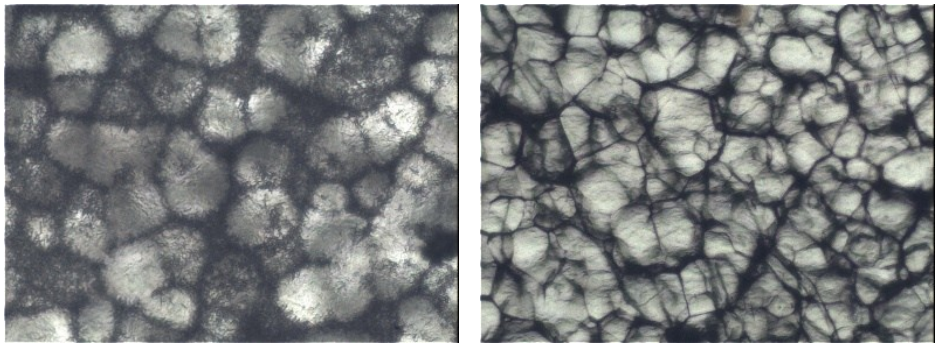

(a) **(b)**

Figure 6. The optical microscopy images of sample 5 films (10% DBC, 20% SA, 70% PP) (a) before and (b) after SA extraction.

The distribution of DBC on the surface of the obtained film was studied using FTIR microscopy in the mid-infrared range. Spectroscopic maps were analysed for the intensity of the band at the maximum position of 1740 cm^{-1}, characteristic solely for DBC. An example result of the measurement of spectroscopic maps is presented in Figure 7.

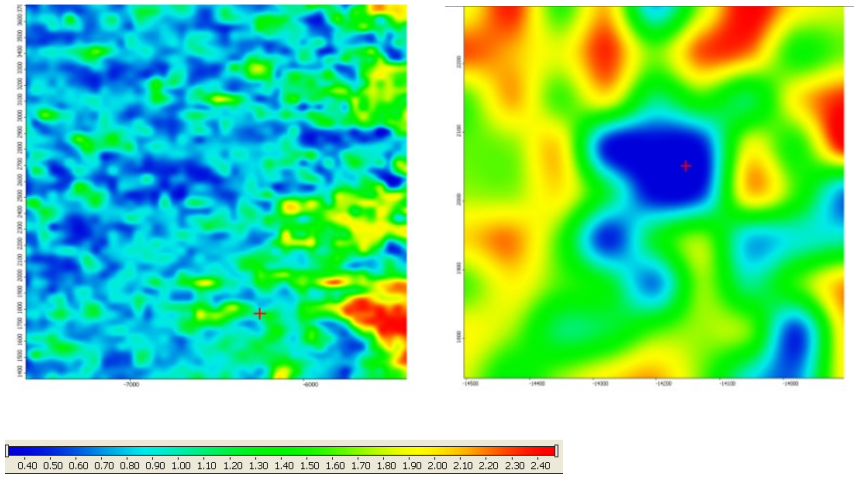

(a) **(b)**

Figure 7. Spectrum map for the 1740 cm-1 band of the sample 5 film surface (10% DBC, 20% SA, 70% PP) (a) before and (b) after SA extraction.

The analysis of the spectroscopic map of the film with the addition of DBC indicates the appearance of the absorption band of carbonyl oscillators of butyric ester groups in the form of weak scattered signals. This is probably related to the blocking of DBC signals by SA (Figure 7a). After the extraction of SA with diisopropyl ether, the signal from DBC increases significantly (Figure 7b). Its distribution indicates DBS presence on the surface of pores formed in the PP films.

Figure 8 presents FTIR spectra of the film treated in 5% KOH and rinsed with water. After the alkaline treatment, the spectra show trace bands at the maximum position of 1100 and 718 cm^{-1}, characteristic of SP, which is formed as a result of the reaction of the hydroxide with the SA remaining in the film.

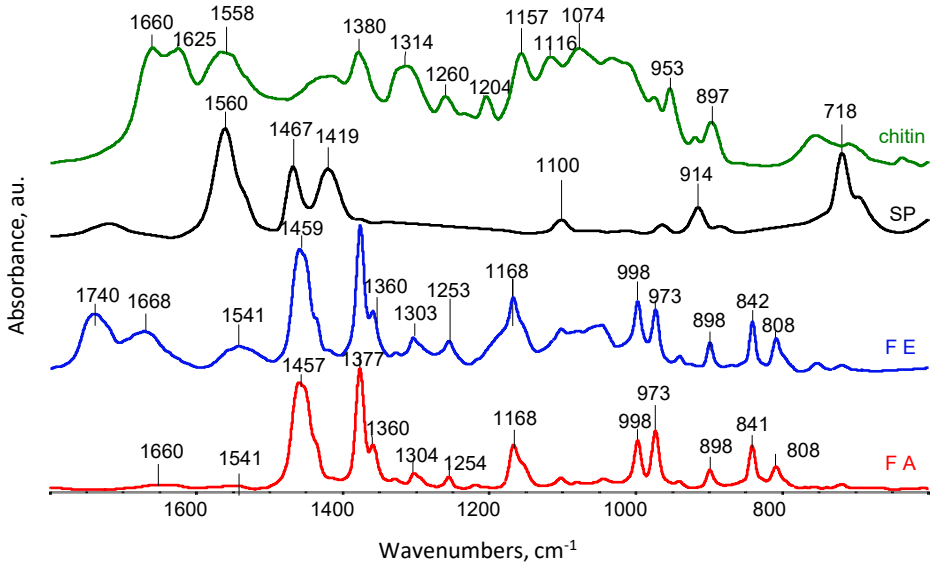

Figure 8. FTIR spectra of chitin, potassium stearate (SP), sample 5 film after SA extraction (FE), and after alkali treatment (FA).

SP is a water-soluble compound, therefore, during rinsing, most of the SP is removed from the film, resulting in a porous structure. Only residues of SP, more strongly bound to the PP matrix, remain in the film. Simultaneously with the transformation of SA during the alkaline treatment, DBC is transformed into chitin, which is evidenced in the FTIR spectra (Figure 8). This is confirmed by the absence of the ester group characteristic band with the maximum position of ca. 1740 cm^{-1} characteristic of DBC. During rinsing with water, DBC and chitin are not removed from the film. Chitin remains in the polypropylene films as demonstrated by the presence of the bands with maximum at ca. 1660, 1074, and 898 cm^{-1}.

Figure 9 shows an example SEM photograph of a film treated with 5% KOH and rinsed with water. The sample 5 film (10% DBC, 20% SA, 70% PP) after alkaline treatment has voids and micro-inclusions of the chitin formed.

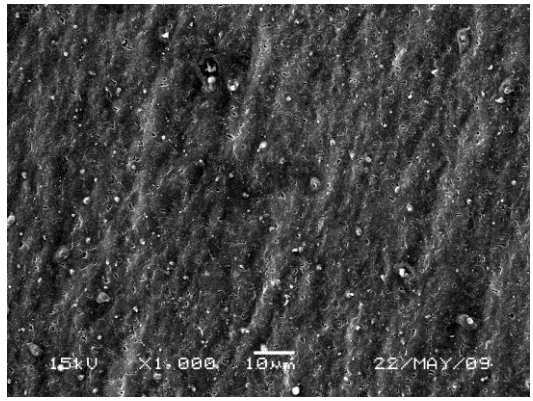

Figure 9. SEM photograph of sample 5 film (10% DBC, 20% SA, 70% PP) after alkali treatment.

4. Conclusions

As a result of the employed procedure, PP films with the addition of DBC and SA were obtained. SA solidifies on the surface of PP in the form of flakes during film formation. As a result of SA extraction in a selective solvent of diisopropyl ether, the flakes were washed out from the surface of the film and partially from its internal part; thus, the film reveals a porous structure. Usage of diisopropyl ether prevents DBC removal from the film, as DBS is not soluble in this solvent. In the next stage, as a result of alkaline treatment, any remaining SA residues react to form SP. At the same time, alkaline treatment causes de-esterification of DBC to regenerate chitin. Finally, rinsing with water causes SP removal, whereas chitin remains untreated.

The obtained results confirm the possibility of production of porous polypropylene film containing chitin and its derivative of DBC, which is foreseen to be used in medicine as a dressing material, a drug carrier, or surgically as a hernia mesh and as a scaffold in tissue engineering.

5. References

[1] Zhang Y, Xin Z; (2007) Isothermal crystallization behaviors of isotactic polypropylene nucleated with α/β compounding nucleating agents. J Polym Sci B Polym Phys 45(5), 590–596. **DOI:** 10.1002/polb.21072

[2] Xiao W, Wu P, Feng J; (2008) Effect of β-nucleating agents on crystallization and melting behavior of isotactic polypropylene. J Appl Polym Sci 108(5), 3370–3379. **DOI:** 10.1002/app.27997

[3] Saha T, Wang X, Padhye R, Houshyar S; (2022) A review of recent developments of polypropylene surgical mesh for hernia repair. OpenNano 7, 100046. **DOI:** 10.1016/j.onano.2022.100046

[4] Sutkar PR, Dhulap VP; (2025) Advancements in polypropylene biodegradation: a comprehensive microbial and analytical review. Sustainable Chem Environ 9, 100213. **DOI:** 10.1016/j.scenv.2025.100213

[5] Sorour MA; (2014) Interposition of the omentum and/or the peritoneum in the emergency repair of large ventral hernias with polypropylene mesh. Int J Surg 12(6), 578–586. **DOI:** 10.1016/j.ijsu.2014.04.009

[6] Houshyar S, Sarker A, Jadhav A, Kumar GS, Bhattacharyya A, Nayak R, Shanks RA, Saha T, Rifai A, Padhye R, Fox K; (2020) Polypropylene-nanodiamond composite for hernia mesh. Mater Sci Eng C 111, 110780. **DOI:** 10.1016/j.msec.2020.110780

[7] Sezer UA, Sanko V, Gulmez M, Aru B, Sayman E, Aktekin A, Vardar Aker F, Yanıkkaya Demirel G, Sezer S; (2019) Polypropylene composite hernia mesh with anti-adhesion layer composed of polycaprolactone and oxidized regenerated cellulose. Mater Sci Eng C 99, 1141–1152. **DOI:** 10.1016/j.msec.2019.02.064

[8] Jo S, Chao C, Khilnani TK, Shenoy A, Bostrom MPG, Carli AV; (2024) The infected polypropylene mesh: when does biofilm form and which antiseptic solution most effectively removes it? J Arthroplasty 39(8), S294–S299. **DOI:** 10.1016/j.arth.2024.04.081

[9] Wei D, Huang Y, Liang M, Yang L, Jiao G, Tao Y, Xu L, Zhang T, Ji Z; (2024) Polypropylene mesh coated with hyaluronic acid/polyvinyl alcohol composite hydrogel for preventing bowel adhesion. Int J Biol Macromol 270, 132061. **DOI:** 10.1016/j.ijbiomac.2024.132061

[10] Angolkar M, Paramshetti S, Gahtani RM, Al Shahrani M, Hani U, Talath S, Osmani RAM, Spandana A, Gangadharappa HV, Gundawar R; (2024) Pioneering a paradigm shift in tissue engineering and regeneration with polysaccharides and proteins-based scaffolds: a comprehensive review. Int J Biol Macromol 265, 130643. **DOI:** 10.1016/j.ijbiomac.2024.130643

[11] Rinaudo M; (2006) Chitin and chitosan: properties and applications. Prog Polym Sci 31(7), 603–632. **DOI:** 10.1016/j.progpolymsci.2006.06.001

[12] Pillai CKS, Paul W, Sharma CP; (2009) Chitin and chitosan polymers: chemistry, solubility and fiber formation. Prog Polym Sci 34(7), 641–678. **DOI:** 10.1016/j.progpolymsci.2009.04.001

[13] Jayakumar R, Prabaharan M, Nair SV, Tamura H; (2010) Novel chitin and chitosan nanofibers in biomedical applications. Biotechnol Adv 28(1), 142–150. **DOI:** 10.1016/j.biotechadv.2009.11.001

[14] Mu L, Wu L, Wu S, Ye Q, Zhong Z; (2024) Progress in chitin/chitosan and their derivatives for biomedical applications: Where we stand. Carbohydr Polym 343, 122233. **DOI:** 10.1016/j.carbpol.2024.122233

[15] Szosland L, Janowska G; (1996) The method of preparation of dibutyrylchitin. Patent PL169077 B1.

[16] Szosland L; (1996) Synthesis of highly substituted butyryl chitin in the presence of perchloric acid. J Bioact Compat Polym 11(1), 61–71. **DOI:** 10.1177/088391159601100105

[17] Szosland L; (1997) Di-*O*-butyrylchitin. In: Muzzarelli RAA, Peter MG (eds), Chitin Handbook. Atec, Grottammare, 53–60.

[18] Piełka S, Paluch D, Staniszewska-Kuś J, Żywicka B, Solski L, Szosland L, Czarny A, Zaczyńska E; (2003) Wound healing acceleration by a textile dressing containing dibutyrylchitin and chitin. Fibres Text East Eur 11(2), 79–84.

[19] Błasińska A, Krucińska I, Chrzanowski M; (2004) Dibutyrylchitin nonwoven biomaterials manufactured using electrospinning method. Fibres Text East Eur 12(4), 51–55.

[20] Muzzarelli RAA, Guerrieri M, Goteri G, Muzzarelli C, Armeni T, Ghiselli R, Cornelissen M; (2005) The biocompatibility of dibutyryl chitin in the context of wound dressings. Biomaterials 26(29), 5844–5854. **DOI:** 10.1016/j.biomaterials.2005.03.006

[21] Wawro D, Stęplewski W, Ciechańska D, Krucińska I, Wesołowska E; (2007) The effect of solvent type on the mechanical properties of dibutyrylchitin (DBC). Fibres Text East Eur 15(3), 14–18.

[22] Chilarski A, Szosland L, Krucińska I, Kiekens P, Błasińska A, Schoukens G, Cisło R, Szumilewicz J; (2007) Novel dressing materials accelerating wound healing made from dibutyrylchitin. Fibres Text East Eur 15(4), 77–81.

[23] Błasińska A, Drobnik J; (2008) Effects of nonwoven mats of Di-*O*-butyrylchitin and related polymers on the process of wound healing. Biomacromolecules 9(3), 776–782. **DOI:** 10.1021/bm7006373

[24] Schoukens G, Kiekens P, Krucińska I; (2009) New bioactive textile dressing materials from dibutyrylchitin. Int J Cloth Sci Technol 21(2–3), 93–101. **DOI:** 10.1108/09556220910933817

[25] Jang SI, Mok JY, Jeon IH, Park KH, Nguyen TTT, Park JS, Hwang HM, Song MS, Lee D, Chai KY; (2012) Effect of electrospun non-woven mats of dibutyryl chitin/poly(lactic acid) blends on wound healing in hairless mice. Molecules 17(3), 2992–3007. **DOI:** 10.3390/molecules17032992

[26] Biniaś D, Biniaś W, Machnicka A, Janicki J, Hałuszka P; (2017) Formation and properties of DBC/PLA microfibres. Prog Chem Appl Chitin Deriv 22, 5–13. **DOI:** 10.15259/PCACD.22.01

[27] Hedrick SA, Chuang SSC; (1998) Temperature programmed decomposition of polypropylene: *in situ* FTIR coupled with mass spectroscopy study. Thermochim Acta 315(2), 159–168. **DOI:** 10.1016/S0040-6031(98)00283-4

[28] Van de Velde K, Kiekens P; (2004) Structure analysis and degree of substitution of chitin, chitosan and dibutyrylchitin by FT-IR spectroscopy and solid state ^{13}C NMR. Carbohydr Polym 58(4), 409–416. **DOI:** 10.1016/j.carbpol.2004.08.004

[29] Binias D, Boryniec S, Binias W, Włochowicz A; (2006) Alkaline treatment of dibutyrylchitin fibres spun from polymer solution in ethyl alcohol. Fibres Text East Eur 14(3), 12–18.

[30] Jahanmardi R, Saberi M, Fathi M; (2020) Preparation of thymolphthalein stearate and appraisement of its efficacy as an antioxidant for polypropylene. Front Chem Res 2, 10–17. **DOI:** 10.22034/FCR.2020.117673.1014

[31] Socrates G; (2004) Infrared and Raman characteristic group frequencies. 3rd ed. John Wiley & Sons, Chichester/New York.